

Article

Potassium Carbonate Supported on γ -Alumina Sorbent Regeneration in Fluidized Bed Reactor for Carbon Dioxide Capture Technology

Chatiya Tripoonsuk¹, Thanjira Maneewatthanakulphol¹, Waranya Khantiudom¹,
Benjapon Chalermssinsuwan^{1,2}, Pornpote Piumsomboon^{1,2,*}

¹ Fuels Research Center, Department of Chemical Technology, Faculty of Science, Chulalongkorn University, 254 Phayathai Road, Pathumwan, Bangkok 10330, Thailand,

² Center of Excellence on Petrochemical and Materials Technology, Chulalongkorn University, 254 Phayathai Road, Pathumwan, Bangkok 10330, Thailand

E-mail: ^achatiya.t@hotmail.com, ^{b,*}pornpote.p@chula.ac.th (Corresponding author)

Abstract. Nowadays, the world is facing severe climate change due to the rapid increase in the world population and the continuing growth of the economy and industry. These lead to substantial greenhouse gas emissions into the atmosphere, especially carbon dioxide, which causes global warming. Thus, carbon dioxide (CO₂) capture becomes an essential technology for mitigating adverse effects on the atmosphere. The solid sorbent is an appropriate alternative for CO₂ capture because it is cheap, environmentally benign, and recyclable. In this study, solid-sorbent regeneration using potassium carbonate supported on gamma-alumina in a fluidized bed reactor was investigated. The effects of operating variables of solid sorbent regeneration were studied by varying the temperatures of 100, 200, and 300 degrees Celsius and pressures in the range from 0 to 1 atmospheric pressure. The results showed that regeneration temperature had a positive effect and initial pressure had a negative effect on the sorbent regeneration, respectively. The sorbent regeneration can be enhanced by increasing the regeneration temperature and decreasing the initial pressure. The optimal condition for sorbent regeneration was at the temperature of 300 degrees Celsius and initial pressures of 0.35 bar. Kinetic studies of the sorbent regeneration were also conducted, and obtained a pseudo-second-order model to be the best-fit model.

Keywords: Carbon dioxide capture, regeneration, potassium carbonate, gamma-alumina, fluidized bed reactor.

ENGINEERING JOURNAL Volume 25 Issue 4

Received 4 December 2020

Accepted 29 December 2020

Published 30 April 2021

Online at <https://engj.org/>

DOI:10.4186/ej.2021.25.4.45

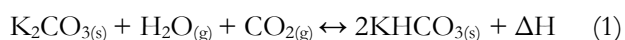
This article is based on the presentation at The 29th Thai Institute of Chemical Engineering and Applied Chemistry Conference (TICAE 2020) in Bangkok, 1st-2nd June 2020.

1. Introduction

Climate change is one of the world's most pressing challenges. Human activities are responsible for almost all of the increase in greenhouse gases in the atmosphere over the last 150 years. For the significant greenhouse gas, the global average concentration of carbon dioxide (CO₂) reaches 407.8 parts per million in 2018, up from 405.5 parts per million (ppm) in 2017. Therefore, this motivates many countries to turn their attention and be aware of the greenhouse gas effects in various fields. Since the United Nations Framework Convention on Climate Change (UNFCCC) has become the most recent and vital international convention to regulate greenhouse gas emission country by country [1], this convention reflects the urgency and high priority for solving climate change by reducing the CO₂ emission including prevention of the adverse effects to human beings.

CO₂ capture technologies are those to separate CO₂ from gases produced in electricity generation and industrial processes. These technologies can be classified into three groups, which consist of pre-combustion, oxyfuel combustion, and post-combustion technologies. The post-combustion technologies are the appropriate alternative since it has an excellent performance without the need to modify the considered process [2]. A variety of post-combustion CO₂ separation technologies are commercially available, for instance, liquid absorption, membrane separation, and dry solid adsorption. Among these, amine liquid absorption is the technology that has been widely implemented in industries. However, the amines have weaknesses in thermodynamic properties, corrosivity, and toxicity [3]. The membrane separation is expensive. Thus, dry solid adsorption becomes an attractive alternative for CO₂ capture since it is inexpensive and environmentally benign.

Potassium carbonate supported on gamma-alumina (K₂CO₃/γ-Al₂O₃) solid sorbent is an outstanding alkali metal comparing to the other alkali and alkali earth metals. The gamma-alumina enhances the adsorption of CO₂ on the sorbent by increasing specific surface areas to accommodate distributed active metal and improves the physical properties of the sorbent [4]. The adsorptive reaction of CO₂ by K₂CO₃/γ-Al₂O₃ is reversibly exothermic and occurs under atmospheric pressure, as shown in Eq. (1)



Sorbent regeneration can be performed by a temperature swing method or pressure swing method where the change of the process condition shifts the equilibrium backward, as shown in Eq. (1). The application of heat to raise the temperature is the conventional method to convert potassium bicarbonate (KHCO₃) to K₂CO₃, but this is an intensive energy-consuming process. On the other hand, the application of pressure reduction is a low energy-consuming process. When the pressure decreases, the reaction shifts backward

to increase the mole of CO₂ and H₂O [5]. The spent sorbents then become active again. In reality, since the sorbent has alumina as a support material, the metal carbonate also reacts with the support materials and forms a complex compound. In this case, it was potassium dawsonite (KAl(CO₃)₂(OH)₂). The potassium dawsonite is a non-CO₂ adsorbing compound, and it is high thermal stability. Thus, to decompose the compound, it requires an even higher amount of energy to convert the spent K₂CO₃ sorbent back to the active K₂CO₃.

The prepared adsorbent, K₂CO₃ support on γ-Al₂O₃, was employed to adsorb CO₂ in the flue gas. The adsorption of CO₂ produced KHCO₃ and the complex compound or potassium dawsonite compound as the other product on the sorbent. Therefore, to fully recover spent solid sorbents with low input energy, the adsorption process has to be operated so that KHCO₃ is the only component formed. It is necessary to restrict the dawsonite formation in the CO₂ adsorption process [6].

The fluidized bed reactor was the system employed in this study for the adsorption reaction since it provides a high mixing rate, which causes the adsorbent particles and CO₂ to be more exposed and provides a constant temperature distribution throughout the reactor. The regeneration of the spent K₂CO₃/γ-Al₂O₃ sorbent via conventional heat regeneration and depressurization in a fluidized bed reactor has not yet been studied in detail.

The scope of this study was to investigate the effect of the regeneration temperature and initial regeneration pressure on the spent sorbent (K₂CO₃/γ-Al₂O₃) regeneration to determine the optimal condition for solid sorbent regeneration and to develop the kinetic model for the solid sorbent regeneration in the fluidized bed reactor.

2. Experimental Section

This experiment consisted of three parts. In the first part, the K₂CO₃/γ-Al₂O₃ adsorbents were synthesized by impregnation. Then, the 12% (v/v) CO₂ balanced with nitrogen (N₂) was passed through the steam generator and then entered the fluidized bed reactor where the CO₂ was adsorbed in a fluidized bed reactor. The second part involved the characterization of the fresh and spent K₂CO₃/γ-Al₂O₃ adsorbents. The last part was the in situ conventional heat regeneration and depressurized regeneration of the solid sorbents in the reactor.

2.1. Preparation of the K₂CO₃/γ-Al₂O₃ Adsorbents by Impregnation

The potassium-based solid sorbents used in this study were prepared by the conventional impregnation of K₂CO₃ onto γ-Al₂O₃ porous support as shown in Fig. 1. First, 5g of γ-Al₂O₃ were added to an aqueous solution containing 5g of K₂CO₃ in 25mL of deionized water and mixed using a solution shaker at room temperature and a rotational speed of 230 rpm for 24h. Then, the mixture was dried at 105 °C for 24 h in an oven. The dried sample

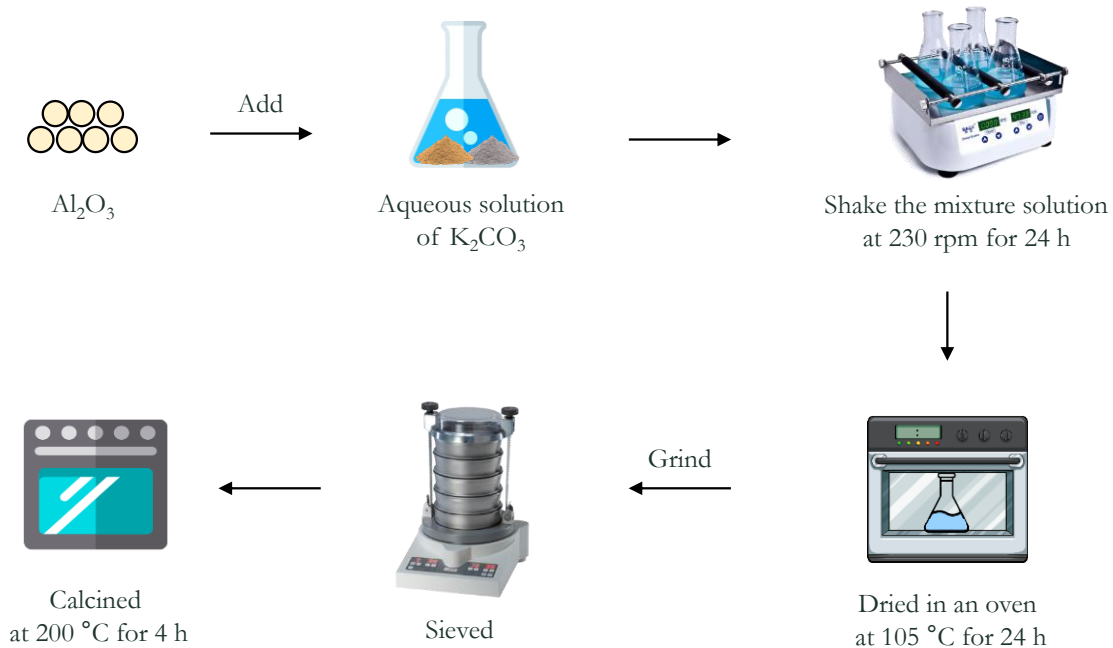


Fig. 1. The outline of the procedure used for preparing the $\text{K}_2\text{CO}_3/\gamma\text{-Al}_2\text{O}_3$ solid sorbent process.

was grained and sieved for collecting different sizes of solid sorbent particles. The samples were calcined in a furnace at 200 °C with the temperature ramping rate at 3 °C/min for 4 h. At this stage, the solid adsorbents were ready for adsorption.

2.2. Characterization of the Fresh and Spent $\text{K}_2\text{CO}_3/\gamma\text{-Al}_2\text{O}_3$ Adsorbents

The nitrogen adsorption–desorption method was used to determine the Brunauer–Emmett–Teller (BET) surface area and total pore volume of the adsorbents using a Micromeritics ASAP 2020 apparatus. Before the measurement, the samples were degassed at 200 °C under vacuum for at least 2 h. Pore size distribution was calculated by a Barrett–Joyner–Halenda (BJH) method.

The amount of alkali metal impregnated on the $\gamma\text{-Al}_2\text{O}_3$ support was determined by X-ray fluorescence (XRF).

The chemical bonding of materials was examined using Fourier transform infrared spectroscopy (FTIR) over the range of 4000–500 cm^{-1} .

The XRD analysis was performed to identify phases presented in the spent and regenerated adsorbents using X-ray diffraction (XRD) using $\text{Cu-K}\alpha$ radiation at room temperature. The analysis was performed at a scanning rate of 0.02 °C/min in 2θ range 10°–80°.

2.3. CO_2 Adsorption and Regeneration in the Fluidized Bed Reactor

Figure 2 shows a schematic diagram of the adsorption and regeneration processes used in this study. The 99.99 % N_2 (A) was fed for removing CO_2 that remained in the system. For the adsorption process, mixed gas with $12 \pm 1\%$ (v/v) CO_2 balanced by nitrogen (B) was fed and controlled

by a mass flow controller (C). The mixed gas was first entered into the steamer (E) and then passed through the adsorbent in the glass column (H) with a flow rate of 0.8 L/min, maintained at a temperature of 60 °C and total pressure 1 atm. The regeneration process using conventional heat and depressurization was investigated as follows. The mass flow controller was closed, and the three-way valve was twisted to connect to a vacuum pump (D). The pressure of the glass column, which contained the spent sorbent, was reduced below 1 atm by the vacuum pump. After that, a circulating pump (G) was started. Finally, the heat was supplied to raise the temperature in the column. The amount of CO_2 in the exiting gas, temperature, and pressure which was released from the glass column, was then detected in real-time by an (I) CO_2 sensor, (J) temperature sensor, and (K) pressure sensor at a sampling rate of 10 samples/min. These data were collected by LabVIEW System Design Software (National Instruments) and recorded in the computer (L). The CO_2 concentration profile was recorded as a breakthrough curve and regeneration curve (M).

3. Results and discussion

3.1. Characterization of Adsorbents

Table 1 shows the BET surface area, pore-volume, pore size, and K_2CO_3 loading of the K_2CO_3 , $\gamma\text{-Al}_2\text{O}_3$, and $\text{K}_2\text{CO}_3/\gamma\text{-Al}_2\text{O}_3$. The fresh $\gamma\text{-Al}_2\text{O}_3$ showed a surface area of 122.2 m^2/g , a pore volume of 0.225 cm^3/g , and pore size of 7.4 nm. The surface area and pore volume of the $\text{K}_2\text{CO}_3/\gamma\text{-Al}_2\text{O}_3$ decreased with an increase in the K_2CO_3 loading. The $\text{K}_2\text{CO}_3/\gamma\text{-Al}_2\text{O}_3$ showed a surface area of 41.5 m^2/g , a pore volume of 0.092 cm^3/g , and pore size of 6.4 nm. As a result, the adsorbents with support had higher surface area and porosity than those without

support. That is because γ -Al₂O₃ has a high surface area and porosity, and it enhanced the distribution of K₂CO₃ on the support. The spent K₂CO₃/ γ -Al₂O₃ showed a surface area of 37.1 m²/g, a pore volume of 0.085 cm³/g, and pore size of 6.4 nm. It indicates that surface area and pore volume slightly decreased compared with fresh K₂CO₃/ γ -Al₂O₃ because the molecule of CO₂ and H₂O covered the adsorbent surface.

The potassium-based γ -alumina sorbents were analyzed with X-ray fluorescence analysis (XRF) to measure K₂CO₃ loadings.

It was found that the K₂CO₃ loading on the K₂CO₃/ γ -Al₂O₃ was 40.83 wt%.

For spent K₂CO₃/ γ -Al₂O₃ after regenerated at three different temperatures, viz., 100, 200, and 300 °C, the K₂CO₃ loadings on the adsorbent were 39.56, 38.54 and 38.19 wt%, respectively. From the experimental results, the weight of K₂CO₃ on the sorbent slightly changed when compared with the fresh K₂CO₃/ γ -Al₂O₃. It indicates that the amount of K₂CO₃ in the adsorbent is not leached or lost during the operation.

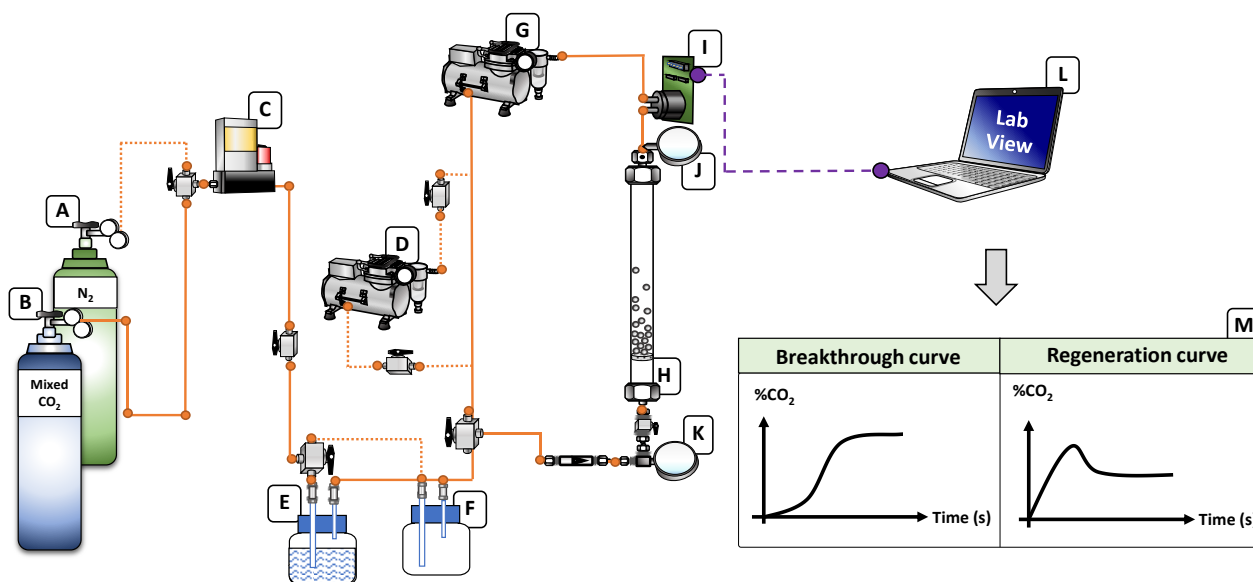


Fig. 2. Schematic diagram of CO₂ fluidization adsorption system and conventional heat - depressurized regeneration system used in this study for (A) N₂ vessel, (B) Mixed CO₂ vessel, (C) Mass flow controller, (D) Vacuum pump (E) Steamer, (F) Vessel (G) Circulating pump, (H) Glass column, (I) CO₂ sensor, (J) Temperature sensor, (K) Pressure sensor, (L) Computer and (M) CO₂ Concentration profile.

Table 1. The physicochemical properties of the solid sorbent.

Sample	S _{BET} ^a (m ² g ⁻¹)	Pore volume ^b (cm ³ g ⁻¹)	Pore size ^c (nm)	S _{ext} ^d (m ² g ⁻¹)	K ₂ CO ₃ loading ^e (wt%)
K ₂ CO ₃	2.5	0.001	2.0	n.d.*	100
g-Al ₂ O ₃	122.2	0.225	7.4	45.8	n.d.*
K ₂ CO ₃ /g-Al ₂ O ₃ -Fresh	41.5	0.092	6.4	40.2	40.83
K ₂ CO ₃ /g-Al ₂ O ₃ -Spent	37.1	0.085	6.4	35.9	40.41
K ₂ CO ₃ /g-Al ₂ O ₃ -Regen-100 °C	38.0	0.086	6.5	36.4	39.56
K ₂ CO ₃ /g-Al ₂ O ₃ -Regen-200 °C	37.8	0.085	6.4	36.3	38.54
K ₂ CO ₃ /g-Al ₂ O ₃ -Regen-300 °C	38.7	0.087	6.5	37.4	38.19

*n.d. = Not determined

^a BET surface area

^b Total pore volume

^c Pore diameter calculated using the BJH method

^d External surface area determined from t-plot curves

^e X-ray Fluorescence

N₂ adsorption-desorption isotherm is shown in Fig. 3. The formation of the hysteresis loop of mesopore type

H3 was observed. Thus, all sorbents were mesopore type IV according to the International Union of Pure and Applied Chemist (IUPAC). Meso-pores are compatible with the size of CO₂ molecules, enhancing the physical sorption on its support framework. The fresh K₂CO₃-impregnated on the γ -Al₂O₃ support sorbent and the spent sorbents did not change the pore type. Hence, the change in the CO₂ adsorption capacity was not likely to be caused by the change in surface area or pore type. The adsorption-desorption isotherms of the regenerated sorbents were similar to the fresh one and had only a slightly lower surface area than the fresh adsorbent [7].

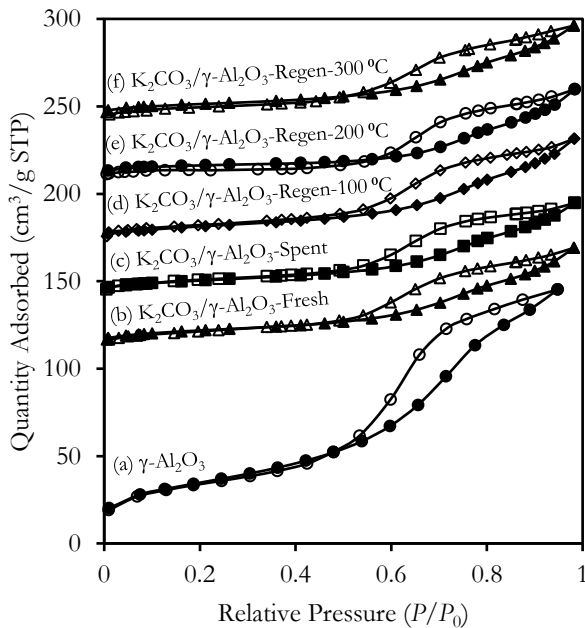


Fig. 3. Nitrogen adsorption-desorption isotherm of the (a) γ -Al₂O₃ support, (b) K₂CO₃/ γ -Al₂O₃-Fresh, (c) K₂CO₃/ γ -Al₂O₃-Spent, (d) K₂CO₃/ γ -Al₂O₃-Regen-100 °C, (e) K₂CO₃/ γ -Al₂O₃-Regen-200 °C and (f) K₂CO₃/ γ -Al₂O₃-Regen-300 °C.

The XRD patterns of fresh, spent, and regenerated adsorbents are shown in Fig. 4. Both K₂CO₃ and KAl(CO₃)₂(OH)₂ phases were presented in the fresh adsorbents. For the fresh K₂CO₃-based adsorbents, the major diffraction peaks shown at 2 θ of 26.2, 30.0, 31.6, 31.6, 32.0, 34.0, 37.7, 38.8, 42.8, and 48.9 were assigned to K₂CO₃ of the monoclinic crystalline phase. While the peaks at 2 θ of 16.0, 21.8, 28.2, 29.7, 32.5, 35.9, and 41.5 were assigned to KAl(CO₃)₂(OH)₂. Additional peaks at 2 θ of 12.9, 24.9, 30.2, 31.5, 39.0, and 40.8 were assigned to KHCO₃ [8].

The XRD peaks of spent and regenerated adsorbents confirmed the presence of KHCO₃ and K₂CO₃ along with KAl(CO₃)₂(OH)₂, respectively. The XRD pattern of sorbents after being regenerated at 100 °C had the peaks at 2 θ of 34.26, 37.64, 39.49, 43.10, and 49.46, which were

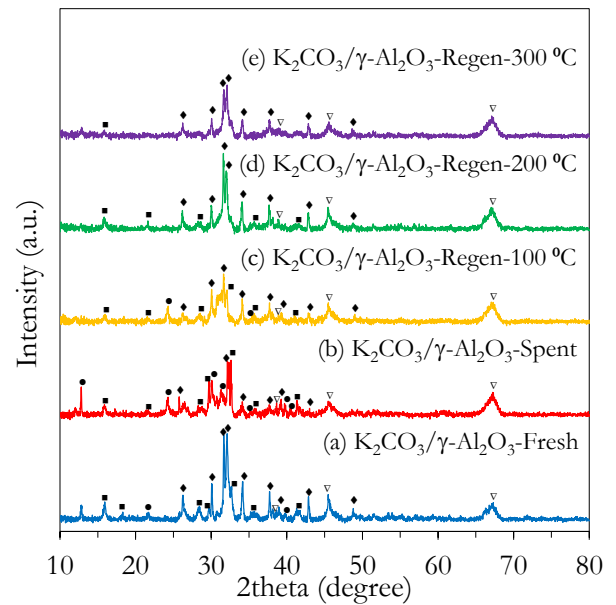


Fig. 4. XRD patterns of (a) K₂CO₃/ γ -Al₂O₃-Fresh, (b) K₂CO₃/ γ -Al₂O₃-Spent, (c) K₂CO₃/ γ -Al₂O₃-Regen-100 °C, (d) K₂CO₃/ γ -Al₂O₃-Regen-200 °C and (e) K₂CO₃/ γ -Al₂O₃-Regen-300 °C [▽, γ -Al₂O₃; ◆, K₂CO₃; ●, KHCO₃; ■, KAl(CO₃)₂(OH)₂].

assigned to K₂CO₃, while peaks at 2 θ of 16.45, 21.89, 28.16, 36.11, and 41.78 were assigned to KAl(CO₃)₂(OH)₂.

After the regeneration at 200 °C, the major peaks of the XRD pattern shown at 2 θ are 26.17, 29.96, 31.93, 33.96, 37.68, 42.89, and 49.09. They were assigned to K₂CO₃, while the peaks at 2 θ of 16.37, 22.18, 28.24, 36.38, and 41.31 were assigned to KAl(CO₃)₂(OH)₂ [9].

K₂CO₃/ γ -Al₂O₃ after regenerated at 100 and 200 °C showed the presence of the same peak position of K₂CO₃ and KAl(CO₃)₂(OH)₂, indicating that only KHCO₃ was converted entirely to the K₂CO₃ and the bicarbonate commences decomposing temperature at 364 K [10]. After the regeneration at 300 °C, only the K₂CO₃ peaks were observed in the XRD patterns [4]. Since KAl(CO₃)₂(OH)₂ is a side product in the adsorption and preparation of adsorbent. The complex compound or Potassium dawsonite compound is produced by potassium aluminum oxide (KAlO₂), potassium carbonate (K₂CO₃), and H₂O, which consists of potassium (K), aluminum (Al), carbon (C), oxygen (O) and hydrogen (H) [9]. Also, the high thermal stability of dawsonite, high input energy are required for the regeneration process. The temperature to decompose the KAl(CO₃)₂(OH)₂ is in the range of 270 - 350 degrees Celsius [6]. Furthermore, it is necessary to restrict the dawsonite formation.

The solid-state FTIR study was conducted for fresh, adsorbed, and regenerated sorbents, as shown in Fig. 5. The peaks that appeared between 1060 and 1506 cm⁻¹ were attributed to the C=O bond. For K₂CO₃, KHCO₃, and KAl(CO₃)₂(OH)₂, the peak appearing between the 740, 865 and 1101 cm⁻¹ region indicated the presence of CO₃²⁻ ions. The peaks appearing between 995 cm⁻¹ indicated the presence of Al-OH tension. The peak that

appeared at 525 cm^{-1} reported the presence of the Al–O group. The peaks observed between 3404 cm^{-1} correspond to the O–H bond stretching band for all of these [11].

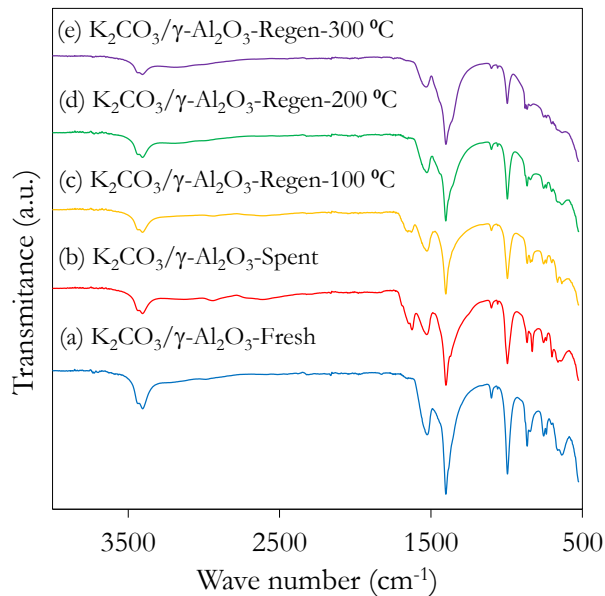


Fig. 5. FTIR spectra of (a) $\text{K}_2\text{CO}_3/\gamma\text{-Al}_2\text{O}_3$ -Fresh, (b) $\text{K}_2\text{CO}_3/\gamma\text{-Al}_2\text{O}_3$ -Spent, (c) $\text{K}_2\text{CO}_3/\gamma\text{-Al}_2\text{O}_3$ -Regen-100 °C, (d) $\text{K}_2\text{CO}_3/\gamma\text{-Al}_2\text{O}_3$ -Regen-200 °C and (e) $\text{K}_2\text{CO}_3/\gamma\text{-Al}_2\text{O}_3$ -Regen-300 °C [∇ , $\gamma\text{-Al}_2\text{O}_3$; \blacklozenge , K_2CO_3 ; \bullet , KHCO_3 ; \blacksquare , $\text{KAl}(\text{CO}_3)(\text{OH})_2$].

3.2. CO_2 Adsorption Studies of $\text{K}_2\text{CO}_3/\gamma\text{-Al}_2\text{O}_3$ Sorbents

A breakthrough curve was plotted in the term of CO_2 concentration (%Volume) concerning time in the riser column, as shown in Fig. 6. The area under the curve could then be integrated to determine the CO_2 capture capacity as $\text{mg-CO}_2/\text{g-K}_2\text{CO}_3$ sorbent (or $\text{mg-CO}_2/\text{g-sorbent}$) using Eq. (2);

$$q = \frac{MW_{\text{CO}_2} P_T F}{RT m_{\text{adsorbent}}} (\text{area } \% \text{CO}_2) \quad (2)$$

where q is the CO_2 capture capacity ($\text{mg-CO}_2/\text{g-sorbent}$), MW_{CO_2} is the molecular weight of CO_2 , P_T is the total pressure, F is the inlet gas flow rate (L/min), R is gas constant, T is the adsorption temperature and $m_{\text{adsorbent}}$ is the mass of active sites on the sorbent (g), respectively.

In this study, the adsorption capacity was found to be $90.46\text{ mg-CO}_2/\text{g-adsorbent}$. The result gave a similar CO_2 capture capacity at about $84\text{--}92\text{ mg CO}_2/\text{g-adsorbent}$ of Jaiboon et al. [12]. Focusing on the 500 seconds of adsorption time, the CO_2 concentration at the outlet of the column had returned to its initial feed concentration since the CO_2 capture capacity of solid sorbent was entirely adsorption [13].

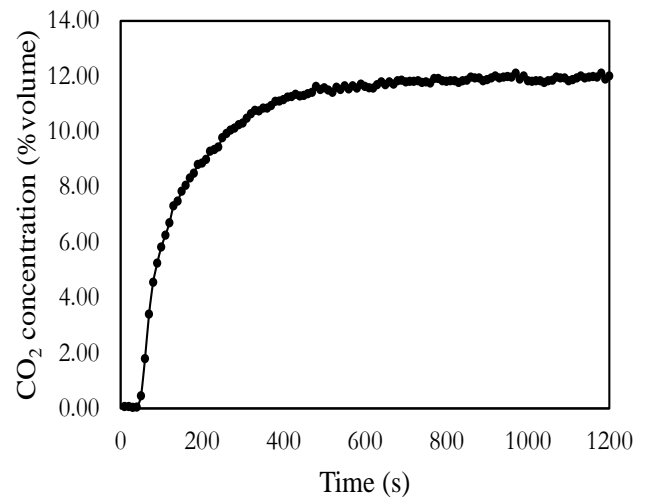


Fig. 6. The breakthrough curve of CO_2 adsorption.

3.3. Sorbent Regeneration Studies of $\text{K}_2\text{CO}_3/\gamma\text{-Al}_2\text{O}_3$ Sorbents

The regeneration of spent sorbents is common practice in various industries where many sorbents are used, and they are easy to regenerate so that the costs due to process operation and waste disposal are reduced. In this research, two sorbent regeneration methods were employed, which were thermal regeneration and depressurization.

Thermal regeneration is a conventional method of sorbent recovery. Temperature swing adsorption is one technology that has been developed based on this approach. The technique gains heat from the adsorption process and then transfers heat to utilize in the regeneration process.[13] The heat treatment can reverse the reaction equilibrium, as shown in Eq. (1) and can bring back the reactants to the original form.

On the other hand, an application of pressure reduction is an alternative method for regeneration. This method consumes less energy, requires shorter regenerating time, and provides high homogeneity to the regenerated sorbent [14]. The % sorbent regeneration is calculated by Eq. (3);

$$\% \text{ Sorbent regeneration} = \frac{m_{\text{released CO}_2}}{m_{\text{adsorbed CO}_2}} \times 100 \quad (3)$$

where $m_{\text{released CO}_2}$ is the mass of CO_2 desorption ($\text{mg-CO}_2/\text{g-sorbent}$) and $m_{\text{adsorbed CO}_2}$ is the mass of CO_2 adsorption ($\text{mg-CO}_2/\text{g-sorbent}$), respectively.

To study the effect of regeneration temperature on the sorbent regeneration, the spent sorbents were heated at three different temperatures, viz., 100, 200, and 300 °C. Figure 7 displays the % sorbent regeneration at these three different temperatures in the fluidized-bed adsorption-regeneration process.

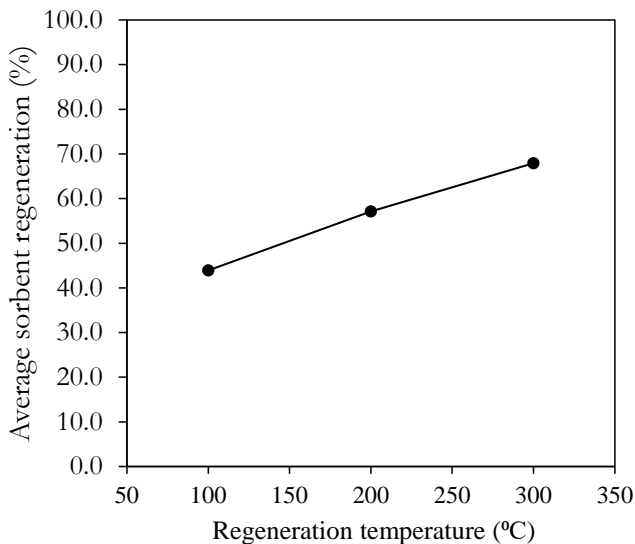


Fig. 7. Effect of different regeneration temperatures on % sorbent regeneration in a fluidized bed reactor.

As shown in the figure, as the temperature for the regeneration increases, the % sorbent regeneration also increases from 43.91% to 67.91%. This is due to the easier decomposition of KHCO_3 (saturated adsorbent) at a higher temperature. It is interesting to note that even at 100 °C, appreciable regeneration of the sorbent (43.91%) occurred and that the % sorbent regeneration increased to 57.14% and 67.91% at higher temperatures (200 and 300 °C), respectively.

It was also found that the sorbent was almost completely regenerated at 350 °C, as displayed by the XRD analysis. For the regeneration at 200 °C, the phases of K_2CO_3 and $\text{KAl}(\text{CO}_3)_2(\text{OH})_2$ were still observed. It indicated that only KHCO_3 was entirely converted to the K_2CO_3 . However, when the regeneration was conducted at 300 °C, only the peaks of K_2CO_3 were observed in the XRD patterns. It is indicated that $\text{KAl}(\text{CO}_3)_2(\text{OH})_2$ was decomposed completely. This confirms that the spent sorbent in this study was completely regenerated [15].

To study the effect of pressure on the sorbent regeneration, the spent sorbents were regenerated at three different pressures, viz., 0.35, 0.61, and 0.88 bar. As shown in Fig. 8, the increase of regeneration initial pressure from 0.35 bar to 0.88 bar reduced the sorbent regeneration from 83.29% to 31.85%. At the 0.61 bar, the sorbent regeneration was found at 53.80%. Due to the unequal moles of the gas phase between the reactant and product, as shown in Eq. (1). When the system pressure was reduced, the reaction equilibrium would be shifted backward to increase the moles of gas species ($\text{CO}_{2(g)}$ and $\text{H}_2\text{O}_{(g)}$) and the pressure in the system [15]. The pressure reduction will initially cause a pressure gradient between the inside and outside of the sorbent pores. The external pressure is less than the internal pressure within the pores. This pressure difference led to the releases of unreacted H_2O on the inner surface and then the CO_2 adsorbed on the sorbent surface. When the initial regeneration pressure

was 0.35 bar, the pressure driving force between the outer and inner pores was higher than that when the initial regeneration pressure at 0.88 bar.

Consequently, the water in the pores and carbon dioxide would be pulled out of the pores with a stronger force (with greater pressure differential). Whereas initial regeneration pressure at 0.88 bar resulted in the water, carbon dioxide, or products in the pores would be pulled out of the pores with a weaker force. So, the sorbent regeneration at 0.88 bar is less than the sorbent regeneration at 0.35 bar [14].

Consider the effects of regeneration temperatures and pressures on % sorbent regeneration, as shown in Figs. 7 and 8. It can be noted that the regeneration temperature shows a positive influence on the % sorbent regeneration, while the regeneration pressure shows a negative impact. Due to the physical phenomenon, the increase in temperature will raise the kinetic energy of the gas molecules. The high kinetic energy molecules can easily escape from the pores of the sorbent; then, the spent sorbents become active again [16].

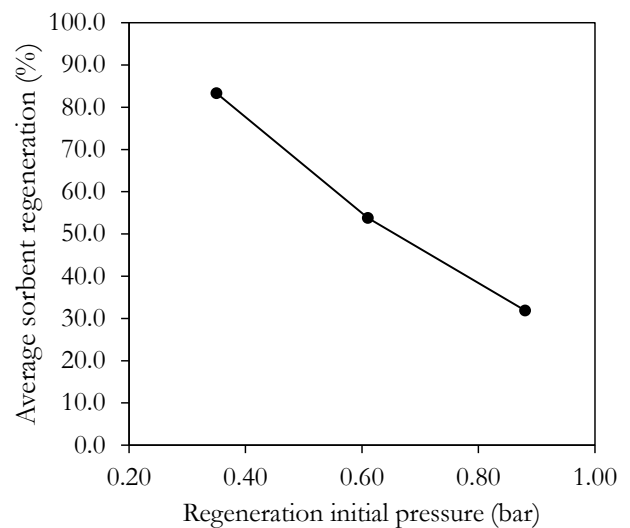


Fig. 8. Effect of different regeneration pressures on % sorbent regeneration in a fluidized bed reactor.

3.4. Optimal Condition of $\text{K}_2\text{CO}_3/\gamma\text{-Al}_2\text{O}_3$ Sorbents Regeneration

The response surface method was implemented to determine the optimal condition of the operating sorbent regeneration process. The method uses a statistical model and explores the relationships between several input variables and one or more response variables. Typically the response variables will be plotted against several independent variables. The contour of the response surface corresponds to the height of the response surface, which can relate to the operating parameters [17]. Figure 9 shows the response surface where % solid sorbent regeneration (Y) was plotted as a function of the regeneration temperatures and initial regeneration pressures. The maximum solid sorbent regeneration was

found at a high regeneration temperature (300 °C) and initial regeneration pressures. (0.35 bar). Due to the curvature of the response surface, the solid sorbent regeneration was improved by increasing regeneration temperature and the decrease of initial regeneration pressures. The regeneration process is an endothermic reaction. The energy is absorbed to break down the bonds of the adsorbed species. The products convert to reactants. In this reaction, the reactants have lower energy than the products when increasing the temperature for regeneration [18]. Resulting in gas molecules had higher kinetic energy. Then, the water or impurities inside the structure of the porous can easily exit from the pores. While the initial regeneration pressure decreases, the reaction can shift backward to increase the moles of CO₂, H₂O, and K₂CO₃ [19].

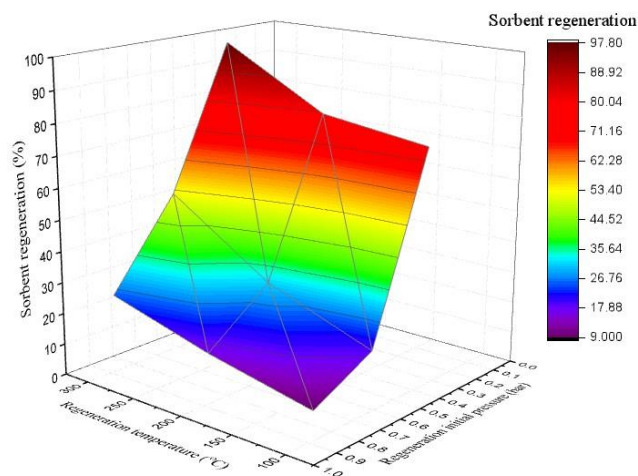


Fig. 9. Response surface of the sorbent regeneration as a function between regeneration temperatures and initial regeneration pressures.

In this work, the kinetic model for solid sorbent regeneration in a fluidized bed reactor was studied using the pseudo-first-order model, the pseudo-second-order model, and the Avrami model. All three models are the most widely applied kinetic models. The pseudo-first-order model was applicable when the absorbate concentration was low and low surface coverage. On the contrary, when the absorbate concentration was high, the pseudo-second-order model was more appropriate. The model is the chemical adsorption resulting from active sites of the adsorption reaction. It is based on the sharing or exchanging of electrons between adsorbent and adsorbate, and it is supposed to be a rate-limiting step. The Avrami model was adapted from a pseudo-first-order model, which is used to describe the complex adsorption process by taking both physical and chemical adsorption into account. This model described more than one reaction mechanism. A typical approach consists of fitting experimental data to a series of kinetic models and selecting the one that provides the best fit.

The pseudo-first-order kinetic model [20] was presented in Eq. (4) and (5);

$$q_t = q_e [1 - \exp^{-k_1 t}] \quad (4)$$

$$\ln(q_e - q_t) = \ln q_e - k_1 t \quad (5)$$

where q_e is the quantity regeneration at equilibrium (mg/g), and q_t is the quantity regeneration at time t (mg/g). k_1 is the rate constant for the pseudo-first-order sorption (min^{-1}). A linear graph with a negative slope is expected from the plot of $\ln(q_e - q_t)$ against t at different concentrations, k_1 and q_{cal} can then be obtained from the slope and intercept, respectively.

The pseudo-second-order kinetic model [21], presented in Eq. (6) and (7);

$$q_t = \frac{k_2 q_e^2 t}{1 + (k_2 q_e t)} \quad (6)$$

$$\frac{t}{q_t} = \frac{1}{k_2 q_e} + \frac{t}{q_e} \quad (7)$$

where k_2 is the rate constant of the pseudo-second-order kinetic equation in mg/g min^{-1} , q_e is the maximum regeneration capacity in mg/g , and q_t (mg/g) is the amount of regeneration at time t . A plot of t/q_t against t was depicted. Then q_e and k_2 can be calculated from the slope and intercepts of the plot.

Equations (8) and (9) express the nonlinear and linear forms of the Avrami kinetic model, respectively [22].

$$q_e [1 - \exp^{-K_{A.V.} t^{n_{A.V.}}}] \quad (8)$$

$$\ln[-\ln(1 - \alpha)] = n_{A.V.} K_{A.V.} + n_{A.V.} \ln t \quad (9)$$

$K_{A.V.}$ is the Avrami constant and $n_{A.V.}$ is the Avrami model exponent of time related to the change in the mechanism of adsorption. $K_{A.V.}$ and $n_{A.V.}$ can be obtained from the intercept and slope of the plot of $\ln[-\ln(1 - \alpha)]$ against $\ln t$.

Calculated parameters of various kinetics models and the validation results were reported in Table 3. This table shows the corresponding kinetic parameters of sorbent regeneration at a regeneration temperature of 300 °C and regeneration initial pressure of 0.35 bar. The best-fit kinetic studies of the sorbent regeneration were considered from the correlation coefficient (R^2) and % error. The equilibrium rate constant of the pseudo-first-order sorption (k_1) was observed to be 0.0096 min^{-1} . The equilibrium rate constant of the pseudo-second-order model (k_2) was $0.000075 \text{ mgCO}_2/\text{g}_{\text{ads}} \text{ min}^{-1}$, and $0.010225 \text{ min}^{-1}$ were assigned to the rate constant of the Avrami model.

In the case of the pseudo-first-order model, the R^2 value was found as 0.9813. While the R^2 value of the pseudo-second-order model was 0.9911, and the R^2 value for the Avrami model was 0.9606. The value of % error of the pseudo-first-order model, the pseudo-second-order model, and the Avrami model were 2.26, 1.60, and 4.41%, respectively.

Table 3. Parameters from the kinetic model of sorbent regeneration.

Kinetic models	$q_{e, \text{model}}$ ($\text{mg}_{\text{CO}_2}/\text{g}_{\text{ads}}$)	k	R ²	Err (%)
Pseudo-first order model	74.38	0.009600 (min^{-1})	0.9813	2.26
Pseudo-second order model	74.89	0.000075 ($\text{mg}_{\text{CO}_2}/\text{g}_{\text{ads}} \text{ min}^{-1}$)	0.9911	1.60
Avrami model	72.74	0.010225 (min^{-1})	0.9606	4.41

It was observed that among the three models, the pseudo-second-order equation gave the best fit to the experimental data since its correlation coefficient (R^2) was very close to unity [23]. The value of % error was also lower than those of the pseudo-first-order model and Avrami model.

These results are suggested that the pseudo-second-order kinetic model provides the best-fit model on sorbent regeneration at regeneration temperature 300 °C and regeneration initial pressure 0.35 bar. This model represents adsorption at high adsorbate loadings [24]. The adequacy of the pseudo-second-order kinetic model can be used to describe the behavior of chemisorption or CO_2 adsorption on potassium carbonate supported on gamma-alumina ($\text{K}_2\text{CO}_3/\gamma\text{-Al}_2\text{O}_3$) [25]. Besides, this model can be used to describe the chemical reaction backward to the reactant.

4. Conclusions

In this study, solid-sorbent regeneration using potassium carbonate supported on gamma-alumina ($\text{K}_2\text{CO}_3/\gamma\text{-Al}_2\text{O}_3$) in a fluidized bed reactor was investigated. The spent adsorbent after CO_2 adsorption can be regenerated by heat treatment and depressurization. However, for the prepared adsorbent, the exothermic equilibrium reaction was not only converted K_2CO_3 to KHCO_3 , but it also produced the byproduct potassium dawsonite compound ($\text{KAl}(\text{CO}_3)_2(\text{OH})_2$), which was the drawback for the regeneration. The high input energy is required in the regeneration process with $\text{KAl}(\text{CO}_3)_2(\text{OH})_2$. It thus was necessary to restrict the dawsonite formation. The XRD analysis confirmed only the K_2CO_3 peaks with the regeneration temperature of 300 °C. Focusing on the main effect of operating parameters, regeneration temperature promoted a positive trend to sorbent regeneration.

In contrast, the initial regeneration pressure shows a negative trend. The initial regeneration pressure expressed a higher impact on the regeneration than the regeneration temperature. However, at high temperatures, the dawsonite complex would be completely decomposed, and the sorbent returned to the original form. Therefore, the optimal condition for sorbent regeneration in this study was at a temperature of 300 degrees Celsius and initial pressures of 0.35 bar. Kinetic studies of the sorbent regeneration were also conducted and obtained a pseudo-second-order model as the best-fit model.

Acknowledgment

The authors gratefully acknowledge the 60/40 Support for Tuition Fee Fund of Chulalongkorn University Graduate Scholarship for supporting the financial support.

References

- [1] B. Metz et al., "Carbon dioxide capture and storage," IPCC Special Report, Policy Stud., 2005.
- [2] A. Samanta et al., "Post-Combustion CO_2 Capture Using Solid Sorbents: A Review," *Industrial & Engineering Chemistry Research*, vol. 51, no. 4, pp. 1438–1463, 2011.
- [3] M. Hasib-ur-Rahman, M. Sijaj, and F. Larachi, "Ionic liquids for CO_2 capture—Development and progress," *Chemical Engineering and Processing: Process Intensification*, vol. 49, no. 4, pp. 313–322, 2010.
- [4] C. Qin et al., "Effect of support material on the performance of K_2CO_3 -based pellets for cyclic CO_2 capture," *Applied Energy*, vol. 136, pp. 280–288, 2014.
- [5] D. Broom, "Characterizing adsorbents for gas separations," *Chemical Engineering Progress*, vol. 114, pp. 30–37, 2018.
- [6] J. V. Veselovskaya et al., "Direct CO_2 capture from ambient air using $\text{K}_2\text{CO}_3/\text{Al}_2\text{O}_3$ composite sorbent," *International Journal of Greenhouse Gas Control*, vol. 17, pp. 332–340, 2013.
- [7] P. Kumar et al., "Metal-organic frameworks for the control and management of air quality: Advances and future direction," *Journal of Materials Chemistry A*, vol. 4, no. 2, pp. 345–361, 2016.
- [8] M. Abunowara and M. Elgarni, "Carbon dioxide capture from flue gases by solid sorbents," *Energy Procedia*, vol. 37, pp. 16–24, 2013.
- [9] O. Martin et al., "Design of hydrothermally-stable dawsonite-based sorbents in technical form for CO_2 capture," *Energy Environ. Sci.*, vol. 7, no. 11, pp. 3640–3650, 2014.
- [10] M. Hartman et al., "Decomposition of potassium hydrogen carbonate: Thermochemistry, kinetics, and textural changes in solids," *Industrial & Engineering Chemistry Research*, vol. 58, no. 8, pp. 2868–2881, 2019.
- [11] L. Fernández-Carrasco et al., "Synthesis and crystal structure solution of potassium dawsonite: An intermediate compound in the alkaline hydrolysis of

- calcium aluminate cements,” *Cement and Concrete Research*, vol. 35, no. 4, pp. 641–646, 2005.
- [12] O.-A. Jaiboon et al., “Effect of flow patterns/regimes on CO₂ capture using K₂CO₃ solid sorbent in fluidized bed/circulating fluidized bed,” *Chemical Engineering Journal*, vol. 219 pp. 262–272, 2005.
- [13] S. Boonprasop et al., “Optimum operating parameters of CO₂ sorption in turbulent fluidized bed regime using potassium carbonate supported on gamma alumina solid sorbent,” *RSC Advances*, vol. 8, no. 69, pp. 39678–39690, 2018.
- [14] S. Boonprasop, B. Chalemsinsuwan, and P. Piumsomboon, “Effect of operating parameters of potassium carbonate supported on gamma alumina (K₂CO₃/γ-Al₂O₃) on CO₂ capture capacity using depressurized regeneration,” *Journal of the Taiwan Institute of Chemical Engineers*, vol. 88, pp. 215–225, 2018.
- [15] S. B. Jo et al., “Regenerable potassium-based alumina sorbents prepared by CO₂ thermal treatment for post-combustion carbon dioxide capture,” *Korean Journal of Chemical Engineering*, vol. 33, no. 11, pp. 3207–3215, 2016.
- [16] C. Zhao, X. Chen, and C. Zhao, “K₂CO₃/Al₂O₃ for Capturing CO₂ in Flue Gas from Power Plants. Part 2: Regeneration Behaviors of K₂CO₃/Al₂O₃,” *Energy & Fuels*, vol. 26, no. 2, pp. 1406–1411, 2012.
- [17] M. Younas et al., “Erratum to: Feasibility of CO₂ adsorption by solid adsorbents: A review on low-temperature systems,” *International Journal of Environmental Science and Technology*, vol. 13, no. 10, pp. 1839–1860, 2016.
- [18] Y. Xie et al., “The effect of novel synthetic methods and parameters control on morphology of nano-alumina particles,” *Nanoscale Res Lett*, vol. 11, no. 1, pp. 259–270, 2016.
- [19] S. Sengupta et al., “Improvement in regeneration properties and multicycle stability for K₂CO₃/Al₂O₃ adsorbents for CO₂ removal from flue gas,” *Energy & Fuels*, vol. 28, no. 8, pp. 5354–5362, 2014.
- [20] Y. Guo et al., “CO₂ sorption and reaction kinetic performance of K₂CO₃/AC in low temperature and CO₂ concentration,” *Chemical Engineering Journal*, vol. 260, pp. 596–604, 2015.
- [21] R. Serna-Guerrero and A. Sayari, “Modeling adsorption of CO₂ on amine-functionalized mesoporous silica. 2: Kinetics and breakthrough curves,” *Chemical Engineering Journal*, vol. 161, no. 1–2, pp. 182–190, 2010.
- [22] A. A. Inyinbor, F. A. Adekola, and G. A. Olatunji, “Kinetics, isotherms and thermodynamic modeling of liquid phase adsorption of Rhodamine B dye onto Raphia hookerie fruit epicarp,” *Water Resources and Industry*, vol. 15, pp. 14–27, 2016.
- [23] N. Jongartklang et al., “Correlations of kinetic parameters with various system operating conditions for CO₂ sorption using K₂CO₃/Al₂O₃ solid sorbent in a fixed/fluidized bed reactor,” *Journal of Environmental Chemical Engineering*, vol. 4, no. 2, pp. 1938–1947, 2016.
- [24] C. Zhao et al., “K₂CO₃/Al₂O₃ for capturing CO₂ in flue gas from power plants. Part 3: CO₂ capture behaviors of K₂CO₃/Al₂O₃ in a bubbling fluidized-bed reactor,” *Energy & Fuels*, vol. 26, no. 5, pp. 3062–3068, 2012.
- [25] S. Sengupta et al., “Circulating fluid-bed studies for CO₂ capture from flue gas using K₂CO₃/Al₂O₃ adsorbent,” *Energy & Fuels*, vol. 32, no. 8, pp. 8594–8604, 2018.





Chatiya Tripoonsuk is currently a Ph.D. candidate at the Department of Chemical Technology, Faculty of Science, Chulalongkorn University, Bangkok, Thailand. She holds a Master of Science in Chemical Technology from Chulalongkorn University and a Bachelor of Engineering in Petrochemical and Polymeric Materials from Silpakorn University. She has a background in both carbon dioxide (CO₂) capture technology and dye adsorption. Her researches focus on carbon dioxide (CO₂) capture technology, carbon dioxide (CO₂) adsorption, solid sorbent regeneration, and circulating fluidized bed.



Thanjira Maneewatthanakulphol received B.Sc. in Chemical Engineering from the Department of Chemical Technology of Chulalongkorn University, Thailand in 2019 with Second Class Honor. She has a background in carbon dioxide (CO₂) capture system of circulation fluidized bed unit.



Waranya Khantiudom received B.Sc. in Chemical Engineering from the Department of Chemical Technology, Chulalongkorn University, Bangkok, Thailand in 2019 with the Second Class Honor, and currently is a M.Sc. student in Chemical Technology, Chulalongkorn University. Her research focus on development a carbon dioxide (CO₂) capture system.



Benjapon Chalermssinsuwan, Ph.D. is an Associate Professor of Department of Chemical Technology at Faculty of Science, Chulalongkorn University. He holds a B.Sc. in Chemical Engineering from Chulalongkorn University and Ph.D. degree in Chemical Technology from Chulalongkorn University. His research interest relates to the several topics including: computational fluid dynamics (CFD) simulation, experimental design and analysis, multiphase flow/fluidization technology and carbon dioxide (CO₂) capture and utilization.



Pornpote Piumsomboon, Ph.D. is a Professor of Department of Chemical Technology at Faculty of Science, Chulalongkorn University, Bangkok, Thailand. He holds a B.Sc. in Chemical Engineering from Chulalongkorn University and Ph.D. degree in Chemical Engineering from University of New Brunswick, New Brunswick, Canada. His research interest relates to the several topics including: carbon dioxide (CO₂) capture and utilization, energy conversion processes, process simulation, and sustainable engineering.